Nordic Hydrology, 7, 1976, 95-114

Seasonal Variability in the Pole-to-Pole Water Vapor Balance During the IGY

Jose P. Peixoto, Richard D. Rosen, and Mao-Fou Wu
Environmental Research & Technology, Inc., Concord, Mass.

A study of the vertically integrated fields of water vapor and its transport on a planetary scale derived from aerological data taken during the IGY (International Geophysical Year) is presented. The focus is upon the seasonal variability in these fields, with maps of the total zonal and the total meridional flux of water vapor given for each of two semester seasons. The analyses are discussed in the light of various climatological and hydrological considerations. Results from the analysis of our aerological data are used to study the balance of water on zonal and planetary scales, and comparisons are made with evidence provided from climatological sources. The aerological approach to the study of the hydrological cycle is seen to be a valuable one.

The role of the atmosphere in the hydrological cycle has long been recognized and been of interest to both climatologists and hydrologists. However, quantitative studies of the gaseous hydrosphere and of its aerial runoff have only been possible in the last two decades, with the develompent of an adequate aerological network.

The first attempts at deriving values for the water vapor flux across latitude zones were based on the utilization of balance requirements for water substance at the earth's surface. In this framework, the flux of water vapor across a latitude φ is assumed to balance the total water transfer occurring at the surface of the earth north of φ through evaporation, precipitation, runoff and water storage. For annual average conditions, matters simplify somewhat so that the meridional transport of

water vapor across a given latitude balances the difference between precipitation and evaporation north of that latitude, since the other terms involved in the yearly hydrological balance can be disregarded (Sellers 1965).

Another approach to evaluating the water vapor flux, the so-called aerological method, is based on the direct use of wind and moisture measurements obtainable from aerological soundings. This method has been described by several authors (see Peixoto 1973) and has been used by the present writers on various occasions. In a previous paper using aerological data (Peixoto 1972), some aspects of the water balance from pole-to-pole were discussed: in particular, the annual mean water vapor transport field. However, the intra-annual variations of both the meridional and the zonal transport fields are also very important for explaining the various hydrological regimes which exist on zonal and global scales and for understanding the influence of the interaction between northern and southern hemispheres on the earth's hydrology. The purpose of the present paper, therefore, is to study and discuss the intra-annual variability of the transport fields on a global basis. The present effort can then be regarded as an extension of the material given in the paper last mentioned above.

The present study is again based on aerological observations from the IGY during which some 450 stations were available over the globe. In spite of some shortcomings concerning the distribution of stations in the basic network, particularly in certain areas of the southern hemisphere, the IGY data may still be regarded as the best available on a global basis. Since, in general, the number of obervations at each station is not very large, data samples were kept at a reasonable size in order to obtain reliable statistics and results. Thus, for our intra-annual study, the year was divided only into two separate seasons: April through September; and January through March plus October through December. This choice of semesters will enable us to deal with the most relevant aspects of the intra-annual variability of the moisture transport fields on a planetary scale.

Since the general formulation of the balance requirements for water vapor in the atmosphere has been given before (eg. Peixoto, 1970), we will restrict our present discussion to a general review of the main points. The basic quantities dealt with are the specific humidity q, the eastward wind component u, and the northward wind component v, with the horizontal vector wind field being given by $\mathbf{v} = u\mathbf{i}_\lambda + v\mathbf{i}_\varphi$. At each station, the time averaged values of the net zonal transport $\bar{F}_\lambda \equiv \overline{qu}/g$ and of the net meridional transport $\bar{F}_\varphi \equiv \overline{qv}/g$ were computed for each semester at 1000, 850, 700, and 500 mb. (On occasion, computations were also made at 300 mb). For this study, observations taken at all times of the day were incorporated. In these expressions, g is the acceleration due to gravity, and the overbar denotes a time average over an interval τ, i.e.

$$\bar{(\ )} \equiv \frac{1}{\tau} \int_{\tau} (\ )\, dt \qquad (1)$$

In the present study, $\tau = 6$ months.

The total mean horizontal transport of water vapor $\bar{\underset{\sim}{Q}}$ above a point on the earth's surface may be written, assuming the atmosphere to be in hydrostatic equilibrium, as

$$\bar{\underset{\sim}{Q}} \equiv \int_0^{p_0} \frac{\overline{qu}}{g}\, dp\, \underset{\sim}{i}_\lambda + \int_0^{p_0} \frac{\overline{qv}}{g}\, dp\, \underset{\sim}{i}_\phi \equiv \bar{Q}_\lambda \underset{\sim}{i}_\lambda + \bar{Q}_\phi \underset{\sim}{i}_\phi \qquad (2)$$

where p_0 denotes surface pressure, and $\bar{Q}_\lambda$ and $\bar{Q}_\varphi$ represent, respectively, the total mean zonal transport and the total mean meridional transport of water vapor in the atmosphere. Similarly, the mean precipitable water content above a given point on the surface may be written as

$$\overline{W} \equiv \int_0^{p_0} \frac{\bar{q}}{g}\, dp \qquad (3)$$

The mean semester values of $\bar{q}$, $\overline{qu}$, $\overline{qv}$, $\overline{W}$, $\bar{Q}_\lambda$ and $\bar{Q}_\varphi$ for each station were plotted on mercator projection maps, and the corresponding fields for each semester were analysed by traditional methods. Grid point values were then extracted from the analyses at every five degrees of longitude and latitude. From these grid point values, the mean zonal fields $[\bar{q}]$, $[\overline{W}]$, $[\bar{Q}_\lambda]$, and $[\bar{Q}_\varphi]$ were computed, where the operator $[(\,)]$ is defined by

$$[(\,)] \equiv \frac{1}{2\pi} \oint (\,)\, d\lambda \approx \frac{1}{72} \sum_i (\,)_i \qquad (4)$$

Mean Precipitable Water

IGY semester maps of the mean moisture content for the whole atmosphere (mean atmospheric storage) were already presented in Figs. 1 and 2 of Peixoto (1972), where a detailed discussion of the analyses was also given. In order to help further our present discussion of the water balance, however, we will summarize here the main points of that previous discussion.

The analyses of $\overline{W}$ show, as expected, that the water content at all latitudes is greater in the summer hemisphere than in the winter hemisphere, with the largest fluctuations occurring in subtropical latitudes. Seasonal variations tend to be more prominent over continents than over oceans, particularly in the case of northern hemisphere continents where the average change in storage between summer and winter is around 0.80 gm cm^{-2}. This stands in contrast to southern hemisphere continents, whose average range in storage between seasons is 0.24 gm cm^{-2}. However, the maximum absolute values of storage do occur in the southern hemisphere, more specifically in South America and in western equatorial Africa, in proximity to the Amazon and Congo river basins. The seasonal variability in these regions is very small.

The difference in seasonal variability between the hemispheres results from the difference in continental coverage, three times larger in the northern hemisphere than

in the southern. As was shown in Table 1 and Fig.4 of Peixoto (1972), the moisture content of the northern hemisphere as a whole is larger than that of the southern hemisphere, due mainly to higher values in northern summer. The difference in continentality is what is also responsible in large part for this behavior, as convective activity tends to be enhanced over land during summer.

Zonal Water Vapor Transport

The spatial distributions of the mean zonal flux of water vapor $\overline{Q}_\lambda$ for the two semesters are shown in Figs. 1 and 2 of the present paper. An inspection of these

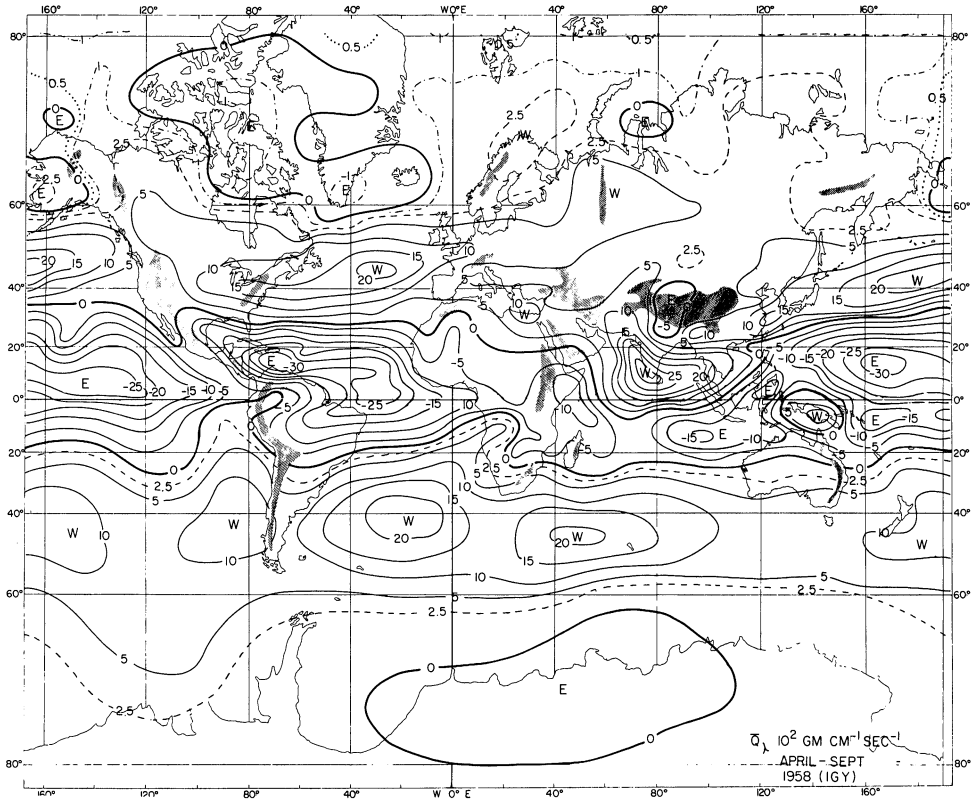

Fig. 1. Map showing the distribution of the vertically integrated mean field of zonal water vapor transport, $\overline{Q}_\lambda(\lambda,\varphi)$, in units of 10^2 g cm^{-1} s^{-1} for the IGY April-September semester. Positive values indicate flow from the west (W).

figures immediately reveals that they reflect the main characteristics of the general circulation in the lower part of the atmosphere, where, of course, water vapor concentration is highest. Thus, two belts of west-to-east water vapor flow extend over the mid-latitude regions in both hemispheres, where westerlies are known to predominate. An almost continuous band of easterly water vapor flow is found over the intertropical and equatorial zones, associated with both the high water vapor content and the strong, persistent easterly winds which prevail in the tropics.

The configurations of the mean fields are by and large similar in the two semesters. However, the profound influence on water vapor transport exerted by local physiography and by land-sea contrast is apparent when northern and southern hemisphere analyses are compared. Thus, the analyses appear much more regular over the southern hemisphere. Highest values of $\overline{Q}_\lambda$ tend to occur over the oceans.

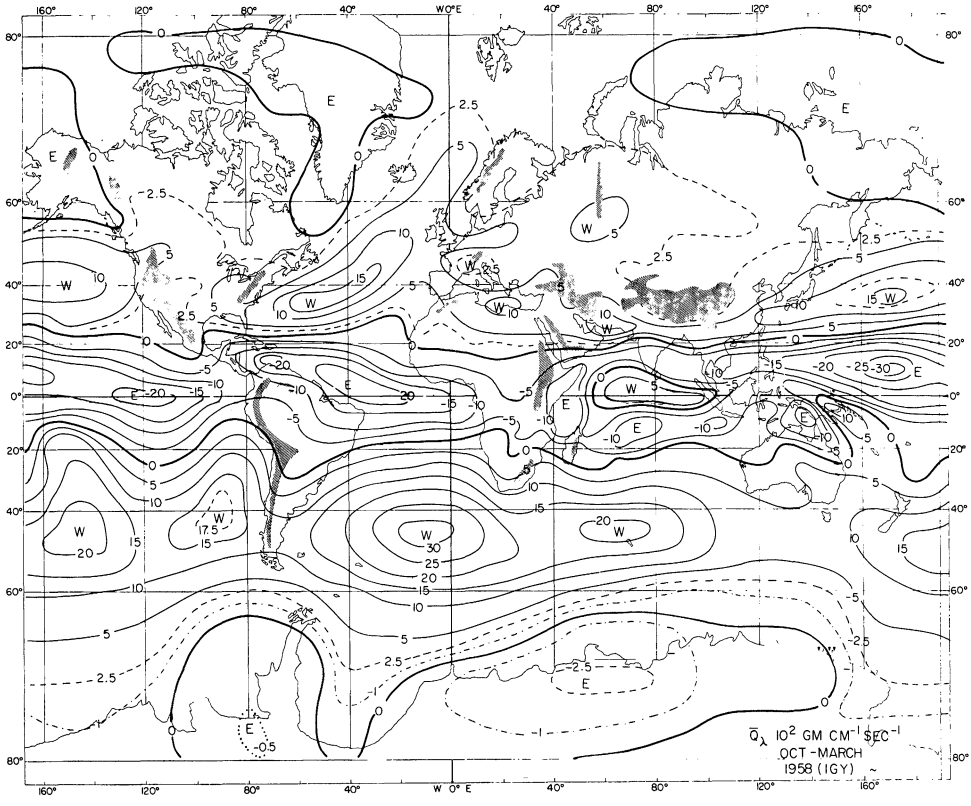

Fig. 2. Map showing the distribution of the vertically integrated mean field of zonal water vapor transport, $\overline{Q}_\lambda(\lambda,\varphi)$, in units of 10^2 g cm^{-1} s^{-1} for the IGY October-March semester. Positive values indicate flow from the west (W).

The westerly circulation of water vapor appears more intense during summer than winter in each hemisphere, due mainly to the higher summer values of humidity. The easterly flow marked by various centers on both sides of the equator does not show large interseasonal changes in intensity. Because of the light winds (doldrums) associated with the equatorial trough, the intensity here is slightly lower than in the bordering regions. Examination of both maps also reveals the influence of monsoon circulations, particularly in the eastern hemisphere, over eastern Africa and south Asia. The summer and winter circulations of water vapor are nearly reversed over these regions. Thus, the intense summer westerly center located over India shifts to the south and weakens considerably in winter.

The westerly circulation belts extend to high latitudes in both hemispheres, though more poleward during the corresponding summer season. In subpolar regions, several easterly centers are to be found in both hemispheres. The centers tend to be more intense in the summer hemisphere.

The analyses presented here show very good agreement over those regions of the globe that have been previously subjected to independent analysis. Reference is here made to vapor flux studies over Australia (Hutchings 1961), Africa (Peixoto and Obasi 1965) and North America (Rasmusson 1967; Bock et. al. 1967).

In order to study the vertical distribution of the zonal transport of water vapor, cross-sections depicting the field of $[\overline{qu}]/g$ are presented in Fig. 3. Both seasonal and annual mean conditions are shown. The cross-sections give evidence of two well developed centers of westerly flow in middle latitudes, surrounded by easterly centers in polar regions and in the intertropical zone. This pattern does not change substantially on a seasonal basis, except for changes in the intensity of the centers. The westerly centers are stronger in the summer semester, whereas the opposite is true for the easterly centers in the tropics.

In the tropics most of the flux occurs in the 1000-800 mb layer, and the main center shifts from one hemisphere to the other, with the winter hemisphere dominating. The situation in middle to high latitudes is very different. Here, the rapid increase of westerly winds with height results in a maximum of zonal vapor flux at higher levels, around 700 mb. The easterly transports which seem to prevail in the polar regions are confined to a shallow layer of the lower atmosphere.

As the figure shows, the mean zonal flux $[\overline{qu}]$ still has relatively high values at 500 mb. Although the specific humidity decreases almost exponentially with height, the zonal wind tends to increase linearly with height. At 500 mb, therefore, it would appear that the strong zonal winds are sufficient to result in the observed substantial water vapor flux. It would seem, therefore, that with regard to the water balance of the atmosphere the contribution to the zonal flux made at higher levels cannot be disregarded. By the same token, the contribution made by the lower layer between 1000 mb and the surface (not included in our present analysis) may be important, particularly in tropical regions where moisture is more abundant.

The zonally averaged values of the vertically integrated mean zonal flux of water

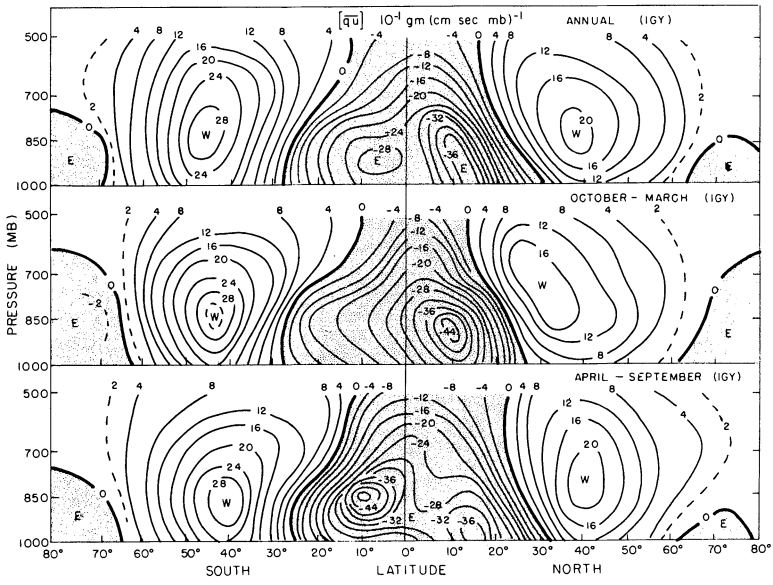

Fig. 3. Meridional cross-sections of the zonally averaged values of the mean zonal transport of water vapor, $[\overline{qu}/g]$, for the IGY yearly and seasonal conditions. Units are 10^{-1} g (cm s mb)$^{-1}$.

vapor for the annual and semester season periods are presented in Table 1 and in the profiles of Fig.4. These profiles provide an easily visualized synthesis of the main characteristics of the zonal transport of water vapor in the atmosphere. The values are positive (westerly) in mid to high latitudes, with a maximum in each hemisphere around 45^0 latitude. The southern hemisphere maximum values exceed those of the northern hemisphere, as we have already indicated. In tropical and equatorial regions, the transport is easterly, with a maximum in each hemisphere surrounding the relative minimum near the equator associated with the light winds there. The intensi-

Table 1 - Distribution of zonally averaged values of total mean zonal transport of water vapor $[\overline{Q}_\lambda]$ for yearly and seasonal data at specified latitudes in units of 10^2 g cm^{-1} s^{-1}.

Lat.	0	5	10	15	20	25	30	35	40	45	50	55	60	65	70	75	80
								Northern Hemisphere									
Year	- 9.23	- 9.98	-11.11	-10.11	-5.90	0.14	4.79	7.18	7.98	7.42	5.85	3.59	1.98	1.34	0.80	0.46	0.11
Apr/Sep	-10.58	-10.20	-10.55	-10.01	-7.56	-2.19	3.80	7.16	9.48	9.45	7.25	4.12	2.15	1.66	0.99	0.78	0.11
Oct/Mar	- 7.04	- 9.76	-11.68	-10.19	-3.26	3.55	6.29	7.23	6.71	5.44	4.26	2.67	1.84	1.15	0.46	0.03	0.12
								Southern Hemisphere									
Year	- 9.23	- 8.41	- 7.00	- 4.33	-0.62	3.31	6.88	10.44	13.45	14.51	12.71	8.48	4.11	1.61	0.50	0.14	0.20
Apr/Sep	-10.58	- 9.03	- 6.80	- 3.68	0.20	3.80	7.14	10.64	14.29	16.85	16.10	12.07	6.81	2.16	0.25	-0.15	0.03
Oct/Mar	- 7.04	- 7.74	- 7.20	- 4.98	-1.06	2.78	6.38	9.49	11.62	12.74	11.39	8.00	3.98	1.53	0.67	0.32	0.23

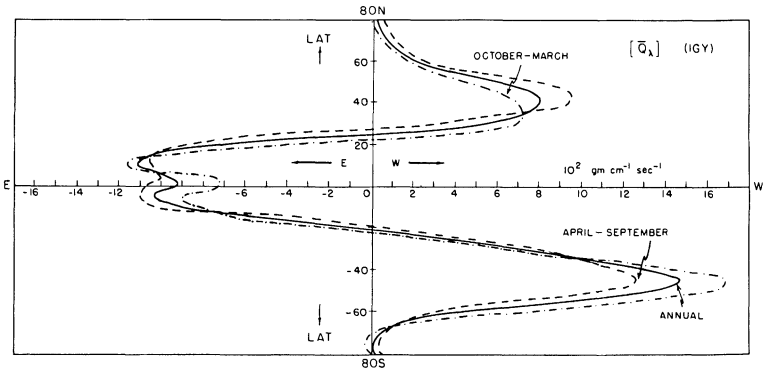

Fig. 4. Meridional profiles of the vertically integrated mean field of zonal water vapor transport $[\bar{Q}_\lambda]$ for the IGY yearly and seasonall conditions. Units are 10^2 g cm^{-2} s^{-1}.

ty of the westerly flux increases in both hemispheres from winter to summer, as the maxima also move to slightly higher latitudes. The easterly maxima are greater during the winter semester in each hemisphere, while the relative minimum over the equator is more pronounced in the northern hemisphere winter.

Meridional Water Vapor Transport

The spatial distributions of the mean meridional flux of water vapor $\bar{Q}_\varphi$ for the two semesters are shown in Figs.5 and 6. The analyses reveal considerable detail, with positive (southerly) transport centers interspersed with negative (northerly) transport centers. The patterns reflect the main characteristics of the general circulation in the lower troposphere and the influence of the inhomogeneity of the earth's surface. The importance of land-sea distribution and of topography is immediately apparent. The most intense centers of meridional flux are found over the oceans and also near the fringes of continents. These latter are associated with diabatic effects arising from thermal land-sea contrasts and display marked reversal with season.

Examination of Figs.5 and 6 reveals a much larger seasonal variability in the nature of the meridional flux of water vapor than was evident for the zonal transport field. The location and intensity of the centers, and occasionally even the sign associated with the direction of the transport, change substantially from winter to summer in both hemispheres. At middle and high latitudes, the net flux is poleward in

both seasons. This transport is accomplished mainly by the baroclinic disturbances which develop along the polar front, and by the large semipermanent subtropical anticyclones found in both hemispheres over the Atlantic, Pacific and Indian Oceans. Thus, in these latitudes the poleward flux is due mainly to the action of the transient and standing eddies in the atmosphere. The intensity of the centers of transport poleward of 30^0 tend to be slightly higher during the winter season of each hemisphere.

In the subtropical and low latitude belts, seasonal differences are much more substantial than at higher latitudes. The seasonal changes observed in Figs.5 and 6 for the intertropical zone form a basic component of the global hydrological cycle, indicating the existence of strong interaction between the hemispheres. In this region, the flux is mostly equatorward, with resulting convergence into the »meteorological

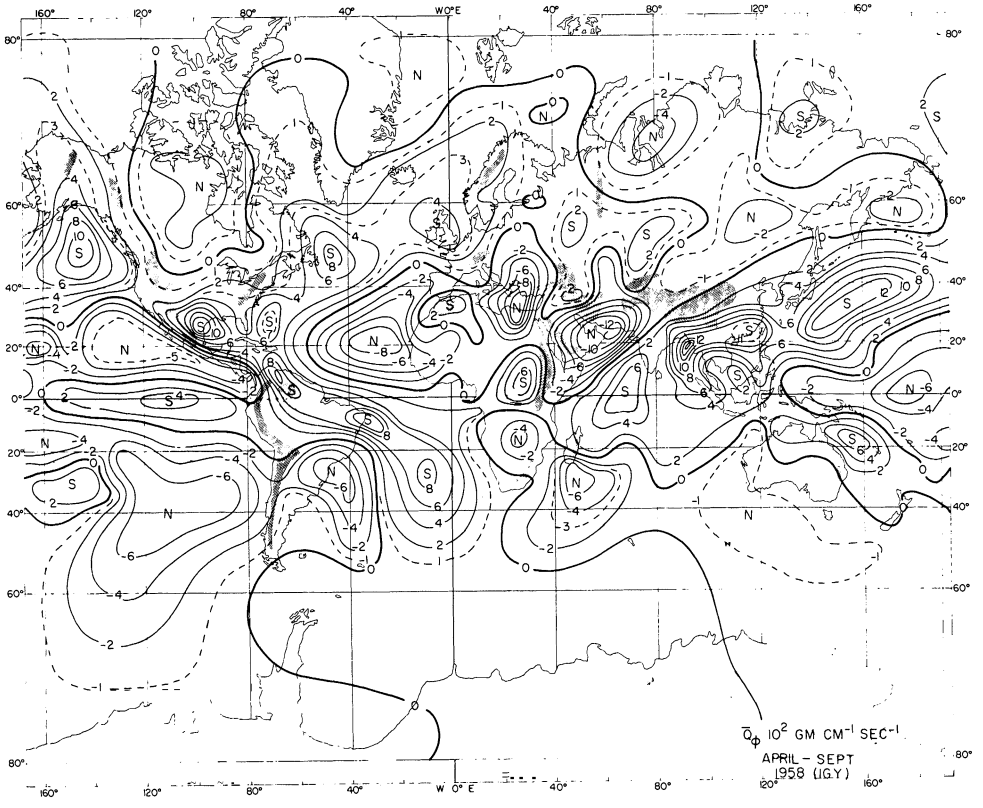

Fig. 5. Map showing the distribution of the vertically integrated mean field of meridional water vapor transport, $\overline{Q}_\varphi(\lambda, \varphi)$, in units of 10^2 g cm^{-1} s^{-1} for the IGY April-September semester. Positive values indicate flow from the south (S).

equator«, the average location of which is about 5°N. However, it shifts from an extreme southern position near 5°S during the southern summer to an extreme northern position near 12°N during the northern summer. There is, concurrently, a strong northward transequatorial flow of water vapor during the northern summer and a somewhat weaker southward flow during the northern winter. For the year as a whole, the net flow is northward across the equator, in conjunction with the positioning of the yearly mean intertropical convergence zone and its concomitant precipitation at about 5°N, as we have already noted.

The distribution and configuration of the various centers in the sub-tropical and tropical belts show the effects of monsoon influence, particularly in the northern hemisphere in the regions over central and eastern Africa, the Arabian Sea, India, south and southeast Asia. The centers change in sign from positive (northward)

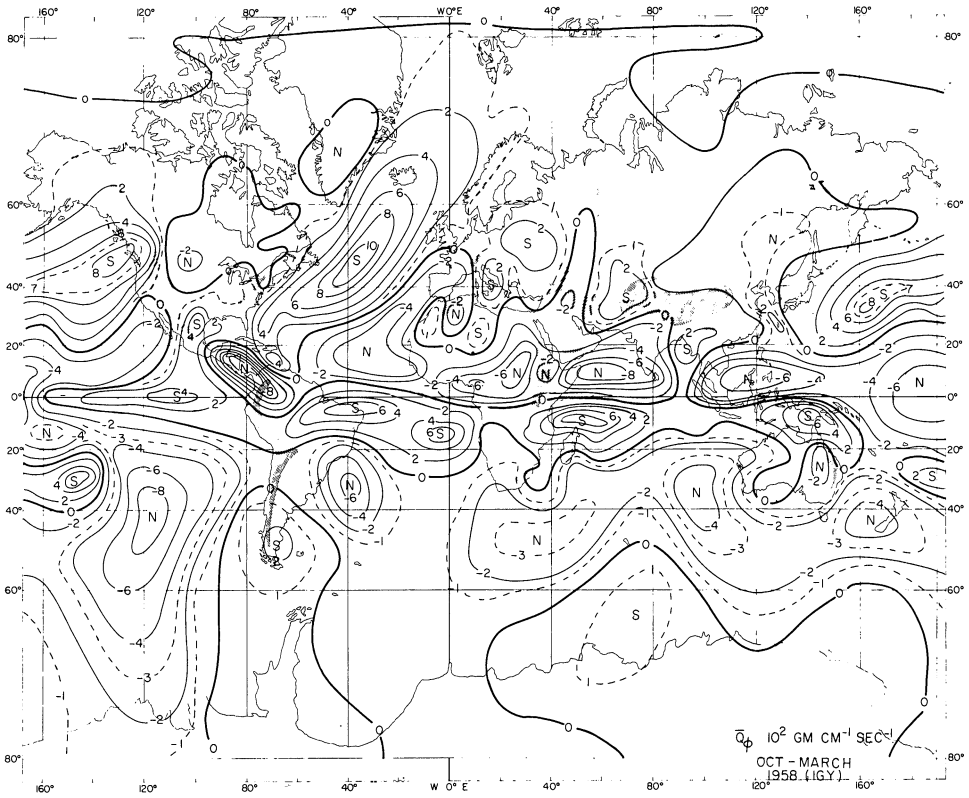

Fig. 6. Map showing the distribution of the vertically integrated mean field of meridional water vapor transport, $\overline{Q}_\varphi(\lambda,\varphi)$, in units of 10^2 g cm^{-1} s^{-1} for the IGY October-March semester. Positive values indicate flow from the south (S).

during the northern summer to negative (southward) during northern winter. Similar, though less marked seasonal effects may be observed in some portions of the southern hemisphere, for example over southern Africa and eastern Australia. Comparison of analyses for both seasons thus reveals that it is the monsoon circulations of the eastern hemisphere which are the large scale features imbedded in the lower branch of the mean Hadley cell most responsible for the intra-annual variability in the meridional transport of water vapor. In sub-equatorial regions, the transport is accomplished mainly by the strong and persistent trade winds of lower levels. Therefore, the role of the Hadley circulation is dominant in transporting water vapor into these lower latitudes, thereby not only maintaining the high moisture contents observed in this zone, but also feeding the precipitation processes which occur there.

Using grid point values obtainable from the maps of $\overline{Q}_\varphi$, mean zonal values of the meridional flux $[\overline{Q}_\varphi]$ have been evaluated. The results for this quantity multiplied by $2\pi a \cos\varphi$ are presented in Table 2 and in profile form in Fig.7, wherein annual and semester season curves are given. These profiles provide a concise format in which the main characteristics of the meridional flux of water vapor may be displayed, and they summarize some of the discussions already presented. The largest positive (northward) values occur around 40°N and 5°S, whereas the largest negative (southward) values occur in the vicinity of 10°-15°N and 40°S. The locations of the extreme values in the tropics change slightly during the year, following the movement of the sun, while the extremes in middle latitudes do not change location appreciably during the year.

So far as the intensity of the extreme values in Fig.7 is concerned, there is a marked seasonal variation over the subtropical and intertropical regions. The meridional flux in these regions is, as we have said, dominated by the lower branch of the mean meridional winter hemisphere Hadley cell, and the intra-annual variability may be understood in this context. The strongest transequatorial flux is accomplished by the southern hemisphere Hadley cell during the April-September semester, when it intensifies and extends into the northern hemisphere. In middle and high latitudes, the seasonal variability in intensity is quite small, the transports being

Table 2 - Distribution of zonally averaged values of the mean meridional transport of water vapor $2\pi a \cos\varphi[\overline{Q}_\lambda]$ across the specified latituted in units of 10^{11} g s^{-1} for yearly and seasonal data.

Lat.	0	5	10	15	20	25	30	35	40	45	50	55	60	65	70	75	80
								Northern Hemisphere									
Year	4.48	- 4.38	- 6.10	-5.06	-1.99	1.23	4.19	6.82	7.14	6.22	4.50	2.57	1.56	1.12	0.41	0.17	0.03
Apr/Sep	11.00	4.62	1.30	-1.82	-0.86	1.20	4.12	6.78	7.07	6.30	5.04	2.70	1.24	0.61	0.23	-0.10	-0.05
Oct/Mar	- 3.08	-13.15	-14.30	-8.31	-2.40	1.27	4.26	6.85	7.23	6.16	4.42	2.50	1.92	1.32	0.68	0.24	0.09
								Southern Hemisphere									
Year	4.48	8.84	7.13	3.25	-1.88	-4.46	-5.44	-6.22	-7.54	-7.10	-5.45	-3.26	-1.22	-0.57	-0.20	-0.10	-0.05
Apr/Sep	11.00	12.85	10.94	1.92	-2.50	-4.81	-5.17	-6.17	-7.11	-6.88	-5.48	-3.60	-1.90	-0.63	-0.26	-0.15	-0.07
Oct/Mar	- 3.08	1.31	3.84	2.68	-0.38	-3.05	-5.60	-6.30	-7.60	-7.20	-5.31	-2.68	-1.01	-0.48	-0.20	-0.10	-0.05

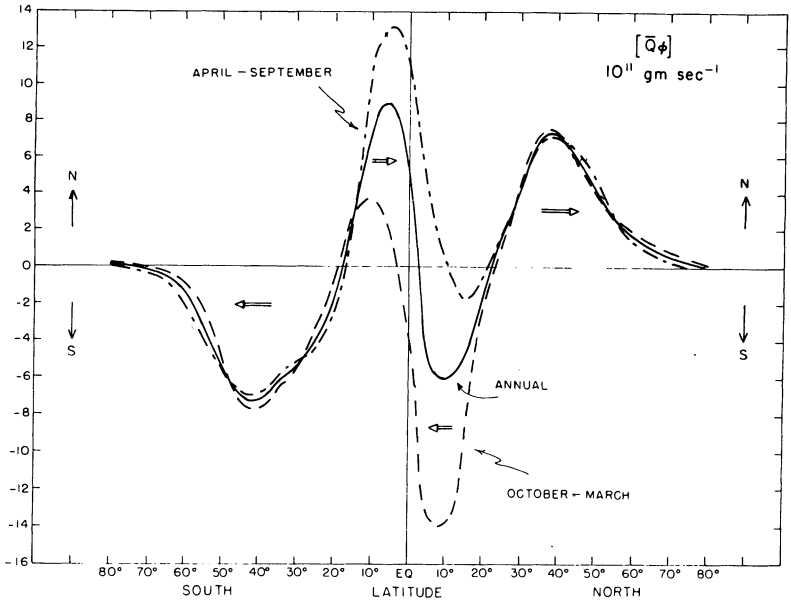

Fig. 7. Meridional profiles of the vertically integrated mean field of meridional water vapor transport, $2\pi a \cos\varphi [\bar{Q}_\varphi]$, across latitude walls in the atmosphere for the IGY yearly and seasonal conditions. Units are 10^{11} g s^{-1}.

slightly stronger during winter. As mentioned earlier, the poleward flux here is accomplished mainly by the transient and standing eddy features of the general circulation, although the smaller contribution made by the indirect mid-latitude cells is also in the same direction. The circulation around the semi-permanent subtropical highs favors a net poleward transport of water vapor from this region, since the poleward flow on the western side contains warmer and moister air than the equatorward flow on the eastern side. Similarly, the transient perturbations which form along the polar front in middle to high latitudes readily effect poleward fluxes of moisture because of the high correlations between v and q associated with their structure.

Zonal and Planetary Water Balance

Most of the discussion that now follows deals with the implications of our previous results for the balance of water on zonal and planetary scales. The discussion will be centered on the presentation of the water vapor balance equation in its various forms

(see Peixoto 1973). The basic time-averaged equation of water balance for a unit mass at a given level may be written as:

$$\overline{\frac{dq}{dt}} = \overline{\frac{\partial q}{\partial t}} + \operatorname{div} \overline{q\underset{\sim}{v}} = s(q) \tag{5}$$

where *s(q)* represents the rate of formation or loss of water vapor per unit mass. In our case, the main sources and sinks of water vapor are associated with evaporation and condensation. Therefore, we may write

$$s(q) = e - c \tag{6}$$

where e is the rate of evaporation and c is the rate of condensation per unit mass. Using a (λ, φ, p, t) coordinate system, Eq. (5) takes the form:

$$\overline{\frac{\partial q}{\partial t}} + \frac{1}{a\cos\phi}\left\{\frac{\partial \overline{qu}}{\partial \lambda} + \frac{\partial}{\partial \phi}\,\overline{qv}\cos\phi\right\} + \frac{\partial \overline{q\omega}}{\partial p} = e - c \tag{7}$$

where a is the mean radius of the earth and $\omega \equiv dp/dt$ is the so-called »vertical p-velocity«. Integration of (5) in the vertical with respect to pressure leads to the general balance equation.

$$\overline{\frac{\partial W}{\partial t}} + \operatorname{div} \overline{\underset{\sim}{Q}} = \overline{E} - \overline{P} \tag{8}$$

where $\overline{E}$ and $\overline{P}$ denote, respectively, the mean evaporation and mean precipitation at the surface of the earth. This equation simply states that the maintenance of the mean water vapor distribution in the atmosphere in light of losses by precipitation and gains by evaporation is accomplished by the divergence of the total water vapor transport field in the gaseous hydrosphere. In spherical coordinates, Eq. (8) may be written as

$$\overline{\frac{\partial W}{\partial t}} + \frac{1}{a\cos\phi}\left\{\frac{\partial}{\partial \lambda}\,\overline{Q}_\lambda + \frac{\partial}{\partial \phi}\,\overline{Q}_\phi \cos\phi\right\} \equiv \overline{E} - \overline{P} \tag{9}$$

For a region of area A bounded by contour l (8) may be transformed using Gauss' theorem into

$$\left\langle \overline{\frac{\partial W}{\partial t}} \right\rangle + \frac{1}{A}\oint (\overline{\underset{\sim}{Q}\cdot\underset{\sim}{n}})\, dl = \langle \overline{E} \rangle - \langle \overline{P} \rangle \tag{10}$$

where $\underset{\sim}{n}$ is the outward normal unit vector on the boundary l and the operator $\langle ( ) \rangle$ represents the areal average with respect to A. When A represents a zonal belt bounded by the latitude circles φ_1 and φ_2. Eq. (10) may be written as

$$\left\langle \overline{\frac{\partial W}{\partial t}} \right\rangle + \frac{1}{A}\oint \{(\bar{Q}_\phi \cos\phi)_2 - (\bar{Q}_\phi \cos\phi)_1\}\, a\, d\lambda = \langle \overline{E} \rangle - \langle \overline{P} \rangle \tag{11}$$

where now $A = 2\pi a^2 (\sin\varphi_2 - \sin\varphi_1)$ is the area of a zonal belt. This equation may be expressed more concisely for hydrological purposes as

$$\overline{\Delta W} + \frac{1}{A}(\overline{F}_2^W - \overline{F}_1^W) \equiv \langle \overline{E} \rangle = \langle \overline{P} \rangle \qquad (12)$$

where $\overline{\Delta W}$ denotes the mean change in water vapor storage and $\overline{F}_i^W$ the mean total transport (i.e., aerial run-off) across a vertical wall at latitude φ_i.

Thus, the excess or deficit of evaporation over precipitation in a zonal belt must be balanced by a change in either the precipitable water over the belt or by a net flux of water vapor through the latitudinal walls, or both. When the change in water vapor storages can be disregarded ($\overline{\Delta W} \approx 0$), as is often the case in dealing with lengthy periods of record, then it must be the net flux which balances the difference between evaporation and precipitation. The same may be said, of course, in connection with (8), thus illustrating directly the importance of the divergence field $\nabla \cdot \underset{\sim}{Q}$ for the balance of water substance.

Maps of the seasonal spatial distributions of the mean fields of water vapor divergence $\overline{\nabla \cdot \underset{\sim}{Q}}$ during the IGY were presented in Peixoto (1972, Figs.8 and 9). There, a detailed discussion of these fields was also given, focussing on the main regional hydrological features of the earth's surface. It was found that by and large the study of the $\overline{\nabla \cdot \underset{\sim}{Q}}$ field constitutes a useful tool for investigations of regional and global hydrological balances. Implications of our results for the divergence fields for aspects of air-sea interaction were also studied. Thus, the present discussion will be confined to the application of the more fundamental flux results, rather than the derived divergence computations, to the study of the mean zonal and planetary water balances on a seasonal basis.

Assuming that $\overline{(\partial W/\partial t)}$ is negligibly small for our purposes, then the zonally averaged form of (9) becomes

$$\frac{1}{a\cos\phi} \frac{\partial}{\partial \phi}([\bar{Q}_\phi]\cos\phi) = [\overline{E}] - [\overline{P}] \qquad (13)$$

Thus, the slope of the profile curves given in Fig.7 can be simply interpreted in terms of the mean zonal value of $[\overline{E} - \overline{P}]$. There is convergence of vapor and thereby an excess of precipitation over evaporation at all latitudes in which $\partial[\overline{Q}_\varphi]/\partial\varphi < 0$, and divergence of vapor where $\partial[\overline{Q}_\varphi]/\partial\varphi > 0$. The extremes of $[\overline{Q}_\varphi]$, where $\partial[\overline{Q}_\varphi]/\partial\varphi = 0$, separate regions of convergence from those of divergence. Therefore, Fig.7 shows that there is vapor convergence ($[\overline{P}] > [\overline{E}]$) at latitudes higher than 40° in both hemispheres and in the equatorial belt. The convergence in this latter region is particularly large, with peak values in the October-March semester. In the zones between 10° and 40° of each hemisphere, there is vapor divergence with a concomitant surplus of evaporation over precipitation. These regions thus represent the main sources of moisture for the gaseous hydrosphere. A portion of this moisture is then exported into more poleward latitudes by the standing and transient eddy perturbations, where it is realized as a precipitation excess associated with the polar fronts of both hemispheres. The other portion of the excess vapor made available in the 10°-40° belts of each hemisphere is transported into the equatorial region and so feeds the

precipitation associated with the intertropical convergence zone. More will be said on this subject later. The seasonal variation of evaporation rates in the tropics between 10^0 and 40^0 is less pronounced in the southern hemisphere than in the northern. However, the individual values are higher in the southern hemisphere because of the greater extent of ocean coverage there.

Using independent climatological estimates of the difference $[\bar{E}] - [\bar{P}]$ for latitudinal belts, the values for $\bar{F}^W \equiv 2\pi a \cos\varphi [\bar{Q}_\varphi]$ given in Table 2 can be tested using equation (12). This has already been done for the annual values of $[\bar{Q}_\varphi]$ and the agreement with the estimate of $[\bar{E}] - [\bar{P}]$ published by Sellers (1962) can be considered to be excellent (Starr, Peixoto, and McKean, 1968, Table 9; Peixoto, 1972, Table 2). Since reliable estimates of $[\bar{P}]$ and $[\bar{E}]$ are not readily available on a seasonal basis, we will confine our present discussion to some qualitative aspects of the seasonal water balance. Preliminary seasonal values of profiles of $[\bar{E}-\bar{P}]$ deduced from the aerological method have been presented previously (Peixoto 1972, Fig.7).

The transequatorial flow of water vapor shows a very marked seasonal variation with a flux into the northern summer hemisphere in the amount of 11×10^{11} g s^{-1}, and a flux out of the northern winter hemisphere in the amount of 3×10^{11} g s^{-1}. For the year as a whole, then, the net influx for the northern hemisphere is about 4.5×10^{11} g s^{-1}. The seasonal variation implies (see Eq. (12)) an excess of precipitation over evaporation in the summer hemisphere, with a much larger excess in the northern hemisphere than in the southern. On an annual basis, as we have noted, the southern hemisphere supplies a substantial amount of moisture to the northern hemisphere. This explains the excess of precipitation over evaporation for this hemisphere on an annual basis (approximately 65 mm year^{-1}; see Palmen and Newton 1969), as well as the reverse condition for the southern hemisphere (Sellers 1965; Newton 1972). The evaporation maps published by Budyko (1963) reveal that the mean northern hemisphere summer value (43 g cm^{-2}) is slightly lower than the value (49 g cm^{-2}) for the northern hemisphere winter semester. This contributes to the large excess of precipitation over evaporation in the northern hemisphere summer, when also the intertropical convergence zone lies furthest to the north and extensive convective precipitation develops over the continents.

Circulation of Moisture and the Hydrological Cycle

On the assumption that the storage term is negligible, zonally averaging Eq. (7) yields

$$\frac{1}{a\cos\phi} \frac{\partial [\overline{qv}]\cos\phi}{\partial\phi} + \frac{\partial}{\partial p} [\overline{q\omega}] = [\overline{s(q)}] \qquad (14)$$

since $[\partial \overline{qu}/\partial\lambda] = 0$. This equation implies that a Stokes water vapor streamfunction Ψ_q can be defined by

$$\frac{\partial \Psi_q}{\partial p} \equiv \frac{2\pi a}{g} \cos\phi \, [\overline{qv}] \tag{15}$$

$$-\frac{\partial \Psi_q}{\partial \phi} \equiv \frac{2\pi a^2}{g} \cos\phi \, [\overline{q\omega}] + F_\ell \tag{16}$$

where F_l measures the flux of liquid water in the vertical. Using the values of the zonal transport $[\overline{qv}]$ measured at various isobaric levels, Eq. (15) can be integrated in the vertical, taking as an obvious boundary condition $\Psi_q = 0$ at the top of the atmosphere. The derived field of Ψ_q thus obtained can be used in equation (16) to deduce the general features of the distribution of the vertical flux of water substance (see Hantel 1974).

Fig. 8 gives meridional cross sections through the atmosphere of the streamlines for the mean meridional transport of water substance for annual and seasonal condi-

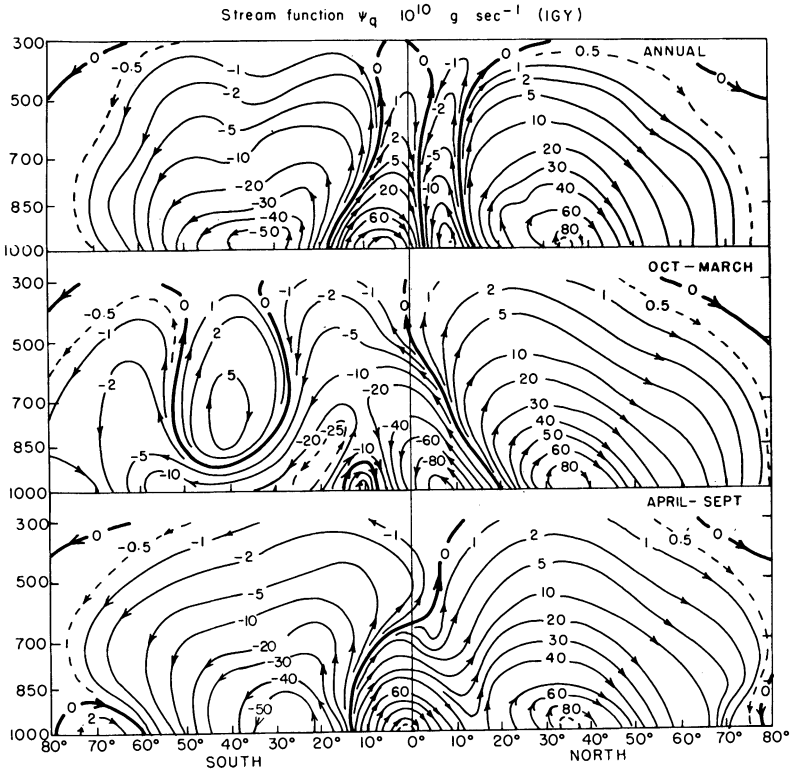

Fig. 8. Streamlines of the mean meridional transport of water vapor in the atmosphere, Ψ_q (φ, p), for IGY yearly and seasonal conditions. Units are 10^{10} g s^{-1}.

tions. Because of the existence of sources and sinks at the earth's surface, the streamlines begin and end there. The manner of presentation made possible through use of the streamline approach is a very attractive one, as the amount of water vapor transported at various heights across latitude walls and the water flux across the surface of the earth are readily viewed. The figure clearly portrays the seasonal variability in water transport, particularly in tropical and equatorial regions. The meridional flux depicted in Fig.8 occurs principally in the lowest part of the atmosphere and the centers of maximum transport are located well within the planetary boundary layer, much below the maximum zonal transport centers.

Those streamlines that begin at the earth's surface indicate the existence of moisture sources with an excess of evaporation over precipitation, while lines that end at the earth's surface reveal the existence of moisture sinks with a precipitation excess. Let us now examine first the October-March cross section. In the northern winter, approximately 200×10^{10} g s^{-1} of water leave the earth's surface between 5°N and 35°N. About 80×10^{10} g s^{-1} are then exported into middle and high latitudes, while the remaining 120×10^{10} g s^{-1} flow equatorward, with most of this contributing to the high precipitation excess between 5°N and 10°S. In the southern summer, there is divergence at the surface between 10°S and 25°S, with part of this flux going north to reinforce the equatorial precipitation and part flowing south towards higher latitudes.

In the April-September semester, there is now a strong divergence of water at the surface between 20°S and 5°S amounting to approximately 160×10^{10} g s^{-1} of which some 120×10^{10} g s^{-1} is fed into the northern summer hemisphere. In turn, of this amount some 90 units feed the precipitation excess in the northern equatorial zone, and the remaining 30 units flow towards regions poleward of 50°N. The source region located between 20°N and 35°N provides about 50×10^{10} g s^{-1}, all of which is exported poleward into higher latitudes, thus reinforcing the moisture originating from the 20°S - 5°S belt and so augmenting the heavy precipitation observed all year round north of 40°N.

The configuration of the streamlines for the annual mean condition shows that an excess of evaporation over precipitation exists between 10°S and 40°S which is considerably large (some 150×10^{10} g s^{-1}). The bulk of this moisture is exported to the northern hemisphere equatorial belt and falls as precipitation in the intertropical convergence zone. Into this zone also flows a small fraction of the 110×10^{10} g s^{-1} made available in the northern hemisphere source zone between 15°N and 35°N. Most of this latter moisture, however, is transported to the more northern sink regions.

The dominant role played by the mean meridional cells in the intertropical and equatorial zones becomes apparent on viewing Fig.8. Thus, the large seasonal variations in the vapor flux discussed above follows closely the seasonal variability of the intensity and latitude of the mean meridional Hadley cells. Winter hemisphere cells are the more intense and represent an effective mechanism for exporting moisture

into the summer hemisphere. This action is stronger for the winter of the southern hemisphere than for the winter of the northern hemisphere, thus leading to the annual net northward transequatorial flow mentioned before. The mechanisms responsible for the transport of water vapor polewards from the subtropical source zones are different however. Here, as we noted earlier, the transports are accomplished largely through the actions of the large-scale standing and transient eddy perturbations of the general circulation.

Final Remarks

Before concluding our present efforts, some remarks of a supplementary nature are in order. These we enumerate below:

(1) The values of the mean zonal transport of water vapor $\overline{Q}_\lambda$ are in general larger than the corresponding ones for the meridional transport, so that the vector transport field $\overline{\underset{\sim}{Q}} = \overline{Q}_\lambda \underset{\sim}{i}_\lambda + \overline{Q}_\varphi \underset{\sim}{i}_\varphi$ has a predominant zonal character. Nonetheless, the meridional component $\overline{Q}_\varphi$ is by far the more important, at least so far as the water balance of the earth and gaseous hydrosphere on a planetary scale is concerned. To be sure, however, $\overline{Q}_\lambda$ does play a very important role in effecting a net water vapor transfer between oceans and continents, because of the configuration and distribution of the continents. On a regional scale, both components of flux can be of equal importance in the study of water budgets.

(2) Considering the hydrosphere *in toto,* there must, on the average, be a compensating meridional flux of water substance in the liquid hydrosphere flowing in opposition to the one observed in the gaseous hydrosphere. Balance considerations thus require a southward transport by the rivers and ocean currents in the middle latitudes of the northern hemisphere, across the equator, and in the southern hemisphere sub-equatorial zone. In the other latitude belts, the total meridional flux of liquid must be northward. Preliminary results indicate that the contribution to the meridional flux of liquid water associated with the north-south component of the run-off from major rivers is detectable, though relatively small when compared to the ocean contribution (Dr. K. Bryan, private communication).

(3) Since the mean change in water vapor storage $\overline{\Delta W}$ may be determined from aerological observations, estimates of $[\overline{P}]$ for various latitude belts may be obtained as a residual in Eq. (12), providing that reliable climatological values of $[\overline{E}]$ are available (Rasmusson in Newell et.al. 1972). This would permit a quantitative description of the broad scale features of the hydrological cycle on a planetary scale. It seems, however, that actual estimates of $[\overline{E}]$ or $[\overline{P}]$ on a monthly, or even on a seasonal, basis are not sufficiently well defined to permit this approach for more than a qualitative description.

(4) Two somewhat different approaches to analyzing the data have been taken here. In the first approach, horizontal analyses are made first at individual levels and then integration in the vertical is performed, as in the case of the streamline functions. These results agree fairly well with the picture obtained through use of the second approach, in which vertical integral quantities (such as $\bar{Q}$) are first computed and then subjected to horizontal analysis. It seems, however, that the latter approach, being more straightforward, is more useful for hydrological purposes.

(5) Although the streamline analyses are very illustrative in depicting some of the main aspects of the circulation of moisture in the atmosphere, they must be viewed cautiously because of the limitations in data sampling and the small number of levels used here. They provide in some sense a metaqualitative image of the mean conditions of an idealized type of flow, which nevertheless shows that the theory of *in situ* evaporation-precipitation cannot be accepted.

(6) In the present work, we have not given the actual numerical results of decomposing the various transport fields into their mean and eddy components, though we have referred to such results on occasion here when discussing the main mechanisms involved in effecting the transports. A recent analysis by Wu (1975) has provided new theoretical grounds on which to point to the large scale atmospheric eddies as being of fundamental importance to the hydrological cycle.

(7) We have confirmed again here the importance of the subtropical and tropical regions for the behavior of the hydrological cycle on a planetary scale. The intensity of the various fields which characterize the dynamics of the gaseous hydrosphere is by far the greater in these equatorial regions. It is, of course, in this area where solar radiation provides the bulk of the energy that sets in motion the hydrological cycle as a whole. Part of this solar energy is redistributed through the hydrological cycle via phase transitions in the water substance. Considering in addition the role of water vapor and clouds in the absorption and disposition of radiant energy, we see that the hydrological cycle is a very important component of the dynamics of climate.

Acknowledgments

The authors are much indebted to Professor Victor P. Starr for his advice and encouragement. Our thanks are also extended to Professor Reginald E. Newell for providing additional data important to this study, and to Ms. Isabelle Kole for drafting the figures. This research has been supported by the Climate Dynamics Research Section, and the Atmospheric Sciences Section, U.S. National Science Foundation under grant no. ATM75-19625.

References

Bock, P., Frazier, H.M., and Welsh, J.G. (1967) *Moisture flux over North America.* Final Rep., Contract Cwb-11313, The Travelers Research Center, Hartford, Conn.

Budyko, M.I. (1963) *Atlas teplovogo balansa Zemnogo Shara.* USSR Glavnaia geofizicheskaia observatoriia, 69. (Text translated by I.A. Donchoo as Guide to the Atlas of the Heat Balance of the Earth; distributed by NOAA, Washington, D.C.)

Hantel, M. (1974) On the display of the atmospheric circulation with streamfunctions. *Mon. Wea. Rev. 102,* 649-661.

Hutchings, J.W. (1961) Water vapor transfer over the Australian continent. *J. Meteor. 18,* 615-634.

Newton, C.N. (1972) Southern hemisphere general circulation in relation to global energy and momentum requirements. Chapter 9 in *Meteorology of the Southern Hemisphere,* Meteorological Monographs 13, A.M.S., Boston, 263 pp.

Newell, R.E., Kidson, J.W., Vincent, D.G., and Boer, G.J. (1972) *The general circulation of the tropical atmosphere, volume 1.* The MIT Press, Cambridge, 258 pp. (see Chapter 5 by E.M. Rasmusson).

Palmen, E., and Newton, C.W. (1969) *Atmospheric circulation systems.* Academic Press, New York, 606 pp.

Peixoto, J.P. (1970) Water vapor balance of the atmosphere from five years of hemispheric data. *Nordic Hydrology 2,* 120-138.

Peixoto, J.P. (1972) Pole-to-pole water balance for the IGY from aerological data. *Nordic Hydrology 3,* 22-43.

Peixoto, J.P. (1973) *Atmospheric vapour flux computations for hydrological purposes.* Reports on WMO/IHD Projects no. 20, World Meteorological Organization, Geneva, 83 pp. (available from UNIPUB, Box 433, Murray Hill Station, New York).

Peixoto, J.P., and Obasi, G.W. (1965) *Humidity conditions over Africa during the IGY.* Sci. Rep. No 7. Planetary Circulations Project, MIT, Cambridge.

Rasmusson, E.M. (1967) Atmospheric water vapor transport and the water balance of North America. *Mon. Wea. Rev. 95,* 403-425.

Sellers, W.D. (1965) *Physical climatology.* University of Chicago Press, Chicago, 272 pp.

Starr, V.P., Peixoto, J.P., and McKean, R. (1968) Pole-to-pole moisture conditions for the IGY. *Pure and Appl. Geoph. 15,* 300-331.

Wu, M.-F. (1975) The role of eddies in atmospheric water vapour transport. *Q.J.R.M.S. 101,* 1019-1022.

Received: 3 March, 1976

Address:
José P. Peixoto,
Richard D. Rosen, and
Mao-Fou Wu,
Environmental Research & Technology, Inc.,
696, Virginia Road,
Concord, Mass-01742, U.S.A.